

Development of a Pharmacokinetic Model That Accounts for the Plasma Concentrations of Conjugated and Unconjugated Bilirubin Observed in a Variety of Disease States

David G Levitt^{1,*}, Michael D Levitt^{2,*}

¹Department of Integrative Biology and Physiology, University of Minnesota, Minneapolis, MN, USA; ²Research Service, Veterans Affairs Medical Center, Minneapolis, MN, USA

*These authors contributed equally to this work

Correspondence: David G Levitt, Department of Integrative Biology and Physiology, University of Minnesota, 6-125 Jackson Hall, 321 Church St. S. E, Minneapolis, MN, 55455, USA, Tel +612 594 0272, Email levit001@umn.edu

Introduction: For a large variety of liver pathologies, the plasma unconjugated (UB) and conjugated (CB) bilirubin concentrations appear to be coupled. For example, in alcoholic cirrhosis, UB and CB are roughly the same over a large range of total bilirubin, requiring an initial massive increase (about 40-fold) in plasma CB to reach the level of UB and then similar increases in UB and CB as the disease progresses. This coupling has been either unrecognized or ignored and this paper is the first attempt to try to explain it quantitatively in terms of known hepatic cell metabolic and membrane transport properties.

Methods: A simplified pharmacokinetic model is developed and applied to a variety of hyperbilirubinemic pathologies. A central feature of the model is based on the recent observation that double knockout of the rat OATP1A and OATP1B hepatic transporters produces a roughly 400-fold increase in plasma CB, indicating that there is a normal rapid recycling of CB from the cell to the plasma with reuptake via OATP. We use the experimental rat K_m of OATP CB transport to show that OATP uptake becomes saturated at relatively low plasma CB concentrations, decreasing uptake, and producing massive (up to 1000-fold) increases in CB in some pathologies. It is assumed that UB and CB are competing for the OATP transporter, producing the increased plasma UB that is observed in “pure” CB pathologies.

Results: The model accurately describes the clinically observed UB and CB for pure UB (Gilbert’s, hemolytic anemia) and CB (Dubin-Johnson, Rotor syndrome, biliary atresia) pathologies as well as in cirrhosis.

Conclusion: This model is a preliminary, first attempt to quantitatively describe UB and CB pharmacokinetics. It is hoped that it will stimulate more detailed measurements and analysis.

Keywords: bilirubin, Dubin-Johnson, Rotor, Gilbert’s, OATP

Introduction

One hundred years have elapsed since van den Bergh¹ described a technique using a diazo reagent to quantitate the plasma concentrations of two species of bilirubin that he named “direct” and “indirect” (the indirect type measurable only in the presence of an accelerant). While it was immediately apparent that direct bilirubin predominated when there was obstruction to bile flow, 40 years elapsed before it was demonstrated that conjugation to glucuronide(s) converted indirect bilirubin to the direct reacting form. While present-day measurements continue to use the basics of van den Bergh’s methodology, it is not commonly recognized that chemical measurements (HPLC) show that the true normal plasma conjugated bilirubin (CB) is only about 0.01 mg/dl, roughly 10% of the 0.1–0.2 mg/dl that is commonly measured as direct reacting bilirubin (see Table 1).² The other 90% consists of a variety of cross-reacting compounds, including unconjugated bilirubin (UB). However, most of

Table 1 Representative Human Plasma Bilirubin Values in Normal and Pathological Conditions. Concentrations are in $\mu\text{mole/Liter}$ and (in Parenthesis) mg/dl . Analytic Chromatographic (HPLC) Values Were Used When They Were Available; Otherwise, the Standard Diazo Assay Values are Used

	Total	Unconjugated	Conjugated	% Conjugated
Healthy (HPLC) ³	6.2 (0.36)	6.0 (0.35)	0.2 (0.012)	3.2
Reference Range (HPLC) ³	2.0 (0.1) – 13 (0.7)	2.0(0.1) – 13 (0.7)	0.06(0.003)- 0.5(0.03)	
Reference Range (Diazo) ⁴	3.5 (0.2) - 20 (1.2)	3(0.15) – 15(0.9)	0.35(0.02) - 4.8(0.28)	
Gilbert's (HPLC) ³	32 (1.8)	31.5 (1.84)	0.29 (0.017)	0.9
Crigler-Najjar I (HPLC) ³	316 (18.5)	316 (18.4)	0.7 (0.04)	0.2
Hemolytic (HPLC) ³	26 (1.52)	25 (1.46)	1 (0.058)	3.8
Chronic alcoholic cirrhosis (Diazo) ⁵	101 (5.9)	49.6 (2.9)	51.4(3.0)	51
Chronic viral hepatitis (Diazo) ⁶	75 (4.4)	27 (1.6)	48 (2.8)	64
Dubin-Johnson (Diazo) ⁷	69 (4.0)	28 (1.64)	40 (2.34)	59
Rotor syndrome (Diazo) ⁸	102 (6.0)	34.2 (2.0)	68 (4.0)	66
Common duct stone (HPLC) ⁹	150 (8.8)	10 (0.58)	140 (8.18)	93
Biliary Atresia (Diazo) ¹⁰	340 (20)	85 (5)	260 (15)	75
Cholestasis of pregnancy (Diazo) ¹¹	14.2 (0.83)	7.4 (0.43)	6.8 (0.4)	48
Primary biliary cirrhosis (Diazo) ¹²	170 (10)	51 (3.0)	120 (7)	70

the increase in direct bilirubin observed in disease states is chemical CB, ie, the artifactual cross-reacting contribution remains relatively constant as CB increases in pathological conditions.² This means that the increase in plasma CB observed in various disease states is enormous, ie, a direct bilirubin of 1.0 mg/dl represents a roughly 100-fold increase over the normal value of about 0.01 mg/dl , a magnitude of increase in plasma concentration not observed for other plasma analytes. Despite immense research effort devoted to bilirubin over the past century, the physiological explanation for such common clinical observations as this massive increase in CB observed in seemingly minor hepatic disease states is not well understood. In this paper, we describe the formulation of a novel pharmacokinetic model that can account for the alterations in CB and UB encountered in a variety of hepatic diseases.

We previously published a comprehensive review that discussed the multiple processes responsible for bilirubin homeostasis in health and disease.² Table 1 summarizes the typical values of the plasma unconjugated (UB) and conjugated (CB) bilirubin in normal and in a variety of pathological conditions. There is a remarkable aspect to these values that we did not comment on in our review and, as far as we are aware, has not been previously discussed. For a “pure” UB pathology such as hemolytic anemia, there is about a 4-fold increase in both UB and CB. This is what is expected for an increase in the total UB production rate since all the UB is converted to CB, and there should be similar increases in cellular UB and CB. (Note: these calculations utilize the true CB normal values measured by HPLC). Similarly, in “pure” UB conjugation pathologies, such as Gilbert’s disease or Crigler-Najjar syndrome, there is, as expected, marked increase in plasma UB and, since there is decreased CB production, minimal change in plasma CB. In contrast, in what would appear to be “pure” CB pathologies due to defects in the biliary excretion of CB where there should be minimal changes in cellular UB (eg, Dubin-Johnson, biliary atresia, biliary obstruction) not only are there massive increases in plasma CB (up to 1000-fold) but, in the chronic, steady-state phase, there are also associated large increases in plasma UB (15-fold). In more non-specific pathologies such as chronic hepatitis or alcoholic cirrhosis, there are again large (250-fold) increases in CB along with smaller increases in UB (8-fold).

These results prompt several interesting questions: 1) What is the pathophysiological process that allows for the enormous (up to 1000-fold) increases in plasma CB, a highly water-soluble, cell membrane impermeable compound that is synthesized only in the liver cell and is normally efficiently excreted in the bile? Such a fractional increase in plasma concentration of any other excretory product is not compatible with life. 2) Why does the plasma UB increase in the pure CB pathologies? 3) The elevated plasma bilirubin in cirrhosis and hepatocellular disease tends to be roughly 50% conjugated and 50% unconjugated. What pathophysiology accounts for the roughly 40-fold more rapid increase in plasma CB versus UB required for CB to reach the UB plasma value (that normally is about 40-fold greater than that of CB), at which point, as liver function deteriorates, plasma CB and UB accumulate in the plasma at roughly the same rate to maintain the similar concentrations of the two types of bilirubin? Seemingly, there must be some process that links the plasma accumulation rates of the two types of bilirubin.

We believe that the answer to these questions is in part provided by the recent observations of Van de Steeg et al¹³ and Iusuf et al¹⁴ that double knockout of the sinusoidal transmembrane organic anion-transporting polypeptides OATP1A and OATP1B produces a roughly 400-fold increase in plasma CB. This finding almost certainly indicates that there is a normal recycling of hepatic CB to the plasma (possibly mediated by MRP3) with reuptake by the hepatocyte cell mediated by OATP.² We assume that pathological increases in intracellular hepatic CB concentration produce an increased rate of efflux from the cell, increasing plasma CB. As shown by measurements in the rat,¹⁵ this OATP mediated cell uptake becomes saturated at relatively low plasma CB, resulting in the huge increases in plasma CB observed in various pathologies. In addition, to explain the increase in plasma UB associated with increases in plasma CB, it is necessary to make the additional assumption that both UB and CB compete for OATP transport into the cell.

Although these assumptions are consistent with clinical observations, we wanted to determine if a kinetic model could be designed that quantitatively mimics the results of Table 1. In section II, we describe a kinetic model that describes the main features of hepatic UB and CB metabolism and transport. In Section III, we apply the model to the conditions in Table 1 that represent relatively “pure” CB or UB pathologies. In section IV, we discuss what pathological changes in the model are required to describe the UB and CB changes seen in conditions such as alcoholic cirrhosis. Finally, in Section V, we discuss the experimental basis for the main assumptions of the model.

Kinetic Model of Hepatic Transport and Metabolism of Unconjugated (UB) and Conjugated (CB) Bilirubin

Figure 1 shows a schematic diagram of our highly simplified model. The crucial component is the recycling of hepatic cell CB with cell efflux via the MRP transporter and reuptake mediated by OATP. OATP is an active transport protein, and it is assumed that the uptake rate is not dependent on the intracellular concentration. Both UB and CB are competing for OATP transport, and we have assumed the simplest possible kinetic description for the two mutually competing substrates:

$$J_{UB} = \frac{V_M}{UB_p + K_{UB} + CB_p \frac{K_{UB}}{K_{CB}}} UB_p \quad J_{CB} = \frac{V_M}{CB_p + K_{CB} + UB_p \frac{K_{CB}}{K_{UB}}} CB_p \quad (1)$$

where UB_p , UB_c , CB_p , CB_c are the plasma and cell UB and CB concentrations, K_{UB} and K_{CB} are the Michaelis-Menton binding constants for UB and CB respectively and V_M is the corresponding V_{max} , assumed to be the same value for UB and CB. In addition to the protein mediated OATP uptake, it is assumed that there is also a passive diffusive UB transport (JP) described by:

$$J_p = P(UB_p - CB_p) \quad (2)$$

where P is the UB permeability constant. The plasma renal clearance (J_R) of CB is described by:

$$J_R = Cl_R CB_p \quad (3)$$

where Cl_R is the CB renal clearance. It is assumed that the CB efflux from the cell to the plasma is linear and does not saturate as the cellular CB concentration (CB_c) increases:

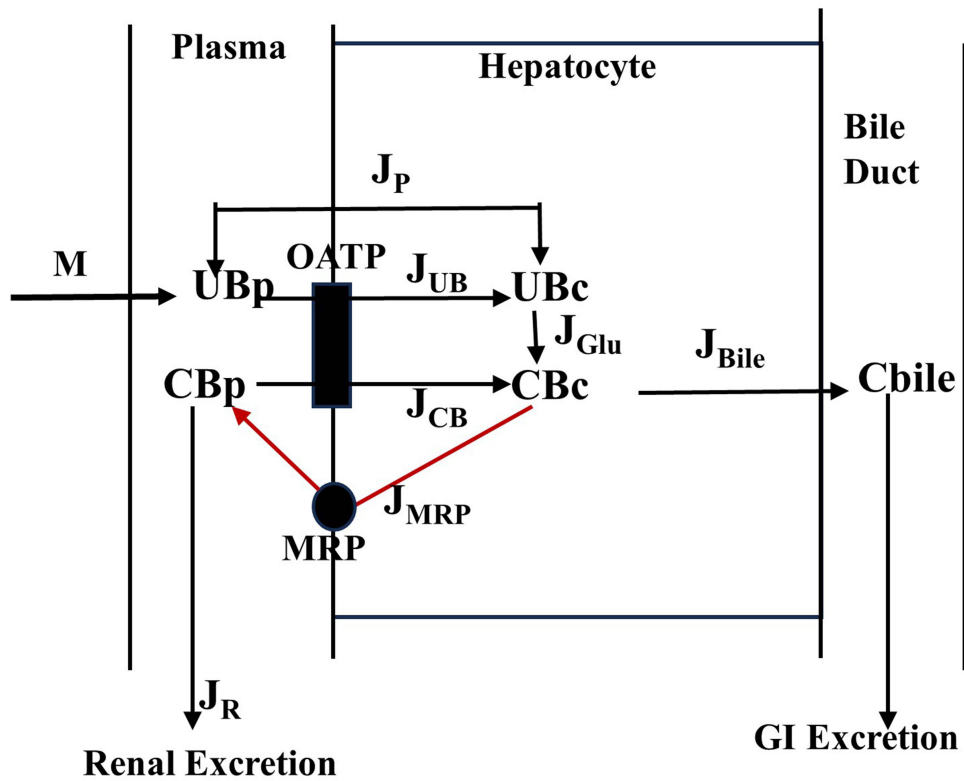


Figure 1 Kinetic model of hepatic bilirubin transport and metabolism. M =rate of bilirubin production. UB_p, UB_c = Unconjugated plasma and cell concentration, respectively. CB_p, CB_c = Conjugated plasma and cell concentration, respectively. J_{UB}, J_{CB} = OATP mediated influx rate of UB and CB, respectively. Concentrations (UB, CB) are in units of mg/dl and fluxes (M, J) are in units of mg/day. **Abbreviations:** J_B diffusive bidirectional flux rate of UB; J_{MRP} protein-mediated efflux rate of CB; J_R , renal excretion of CB; J_{Glu} , rate of glucuronidation of UB; J_{Bile} , rate of biliary secretion of CB.

$$J_{MRP} = R_{MRP} CB_c \tag{4}$$

The rate of glucuronidation of UB and the rate of bile secretion of CB are also assumed to be linear and non-saturable:

$$J_{Glu} = R_{Glu} UB_c \tag{5}$$

$$J_{Bile} = R_{Bile} CB_c \tag{6}$$

where R_{MRP}, R_{Glu} and R_{Bile} are the corresponding rate constants.

It is assumed that the UB and CB concentrations are in a steady state. The steady state equation for plasma UB (=UB_p) is:

$$J_{UB} + J_P - M = 0 = \frac{V_M}{UB_p + K_{UB} + CB_p \frac{K_{UB}}{K_{CB}}} UB_p + P(UB_p - UB_c) - M \tag{7}$$

The plasma CB (=CB_p) steady state equation is described by:

$$J_{CB} + J_R - J_{MRP} = 0 = \frac{V_M}{CB_p + K_{CB} + CB_p \frac{K_{CB}}{K_{UB}}} CB_p + Cl_R CB_p - R_{MRP} CB_c \tag{8}$$

The steady state equation for intracellular UB (=UB_c) is:

$$M - R_{Glu} UB_c = 0 \Rightarrow UB_c = \frac{M}{R_{Glu}} \tag{9}$$

The steady state equation for intracellular CB (=CB_c) is:

$$M - Cl_R CB_p - R_{Bile} CB_c = 0 \Rightarrow CB_c = \frac{M - Cl_R CB_p}{R_{Bile}} \quad (10)$$

For completeness, we should also include a term for reflux directly from the bile to the plasma as may occur, eg, in biliary obstruction. However, for the model in Figure 1, this flux is kinetically identical to an equivalent decrease in J_{Bile} , and, therefore, is not necessary.

Although the physiologically important concentration is the free (not total) concentration, because the bilirubin albumin (plasma) and ligandin (intracellular) binding is poorly characterized, all concentrations in these equations are the total concentration, and it is assumed that the binding constants have been incorporated as part of the transport coefficients and binding constants. All concentrations are in units of mg/dl (see Table 1), fluxes (J , M , V_M) are in units of mg/day, and the flux clearances (P , R , and Cl_R) are in units of dl/day.

Table 2 summarizes all the parameters in the model and the human quantitative numerical values assigned to them. The experimentally known rates are the total rate of bilirubin production ($M = 250$ mg/day) and the renal clearance of CB ($Cl_R = 12$ dL/day).² Also known are the normal plasma UB ($UB_{po} = 0.35$ mg/dl) and CB ($CB_{po} = 0.012$ mg/dl). We have also used the average clinical Rotor syndrome plasma concentrations reported for a large series of cases by Namihisa and Yamaguchi⁸ for UB ($UB_{pr} = 2$ mg/dl) and CB ($CB_{pr} = 4$ mg/dl). The normal intracellular UB and CB are not known and, as a first approximation, we have assumed that the normal cell UB is equal to the normal plasma UB, and the normal cell CB concentration is 10 times the normal plasma CB (see Table 2). The primary effect of these intracellular assumptions is to scale the values of the rate constants R_{Glu} , R_{Bile} and R_{MRP} in Table 2 (so that only their relative values are meaningful) and these assumptions do not significantly change the results shown in the following figures and tables.

All the other model parameters can be directly calculated from these parameters as described below and are summarized in Table 2. The rate constants R_{Glu} and R_{Bile} are determined from eqs. (9) and (10), respectively, using the normal plasma UB

Table 2 Summary of the Normal Human Quantitative Model Parameters and Rate Constants

Symbol	Description	Value	Source
M	Rate of UB synthesis	250 mg/day	Measurement
Cl_R	CB renal clearance	12 dL/day	Measurement
UB_{po}	Normal plasma UB	0.35 mg/dl	Measurement
CB_{po}	Normal plasma CB	0.012 mg/dl	Measurement
UB_{co}	Normal cell UB	= U_{po}	Assumption
CB_{co}	Normal cell CB	= 10 × C_{po}	Assumption
UB_{pr}	Rotor plasma UB	2 mg/dl	Measurement
CB_{pr}	Rotor plasma CB	4 mg/dl	Measurement
R_{Glu}	Normal UB glucuronidation	714 dL/day	Calculation
R_{Bile}	Normal CB bile excretion	2082 dL/day	Calculation
P	Passive UB permeability	151 dL/day	Calculation
R_{MRP}	CB MRP efflux rate	495 dL/day	Calculation
K_{CB}	OATP K_m for CB	0.2 mg/dl	Estimate
K_{UB}	OATP K_m for UB	1.382 mg/dl	Calculation
V_M	OATP V_{max}	1296 mg/day	Calculation

(UBpo) and CB (CBpo) concentrations. Of crucial importance for calculating the model parameters are measurements of the plasma UB (UBpr) and CB (CBpr) in subjects with Rotor syndrome. It has been shown that these individuals have defective OATP hepatic transport, and we have assumed that it corresponds to the model in [Figure 1](#) with OATP absent. Thus, in Rotor syndrome, eqs. (7) and (8) reduce to:

$$P(UBpr - UBcr) - M = 0 \quad (11)$$

$$Cl_R CBpr - R_{MRP} CBcr = 0 \quad (12)$$

where UBpr and UBcr are the plasma and cell UB concentration, respectively, and CBpr and CBcr and plasma and cell CB concentrations in Rotor syndrome. We assume that the defect in OATP in these patients does not alter other cellular functions so that R_{MRP} and the other rate constants and the intracellular UB concentration are normal (ie, $UBcr = UBco$). Thus, P can be determined from eq. 11:

$$P = \frac{M}{UBpr - UBco} = 151 \text{ dl/day} \quad (13)$$

The intracellular CB (= CBcr) concentration in Rotor's syndrome can be determined from eq. (10) using the previously determined parameters from [Table 2](#) ($CBcr = 0.097 \text{ mg/dl}$). Substituting this CBcr into eq. (12) yields the normal value for $R_{MRP} = 494.7 \text{ dL/day}$

The K_m of the mouse OATP1B1 for bilirubin monoglucuronide is 0.005 mg/dl .¹⁵ This measurement is in the absence of albumin and thus corresponds to the free CB binding K_m . Assuming that plasma CB is from 1 to 2% free,¹⁶ this would correspond to a $K_m (=K_{CB})$ in the range of 0.2 to 0.5 mg/dl for the total CB concentration, which is the parameter utilized in the above equations. We have assumed a value of $K_{CB} = 0.2 \text{ mg/dl}$ ([Table 2](#)). The normal plasma UB (UBpo) and CB (CBpo) concentrations were utilized in eq. (7) to find the dependence of V_M on K_{UB} :

$$V_M = \frac{(UBpo + K_{UB} + CBpo \frac{K_{UB}}{K_{CB}})(M - P(UBpo - UBco))}{UBpo} \quad (14)$$

Finally, substituting this V_M into eq. (8), we can solve for the normal value of $K_{UB} = 1.382 \text{ mg/dl}$ and $V_M = 1296 \text{ mg/day}$. This completes the derivation of the model parameters.

Model Fits for Pure UB and CB Pathologies

This model will now be tested for its ability to roughly reproduce the plasma UB and CB concentrations for the pathologies listed in [Table 1](#). We will first consider the case of "pure CB" pathologies (eg, Dubin-Johnson, primary biliary cirrhosis) that result from a defect in CB biliary excretion (J_{Bile} , [Figure 1](#)), defects represented in the kinetic model equations by a pathological decrease of the rate constant R_{Bile} (eq. (6)). [Table 3](#) lists the plasma UB and CB for a range of fractional decreases in R_{Bile} . To produce the 195-fold increase in plasma CB (2.34 mg/dl) seen in Dubin-Johnson ([Table 1](#)) requires that R_{Bile} is decreased to 0.046 of its normal value (a 22-fold reduction). This R_{Bile} decrease also produces a 4-fold increase in the model plasma UB to 1.39 mg/dl, similar to what is observed clinically in Dubin-Johnson ([Table 1](#)). This plasma UB increase results from the competitive inhibition of OATP UB uptake by the increased plasma CB concentration. In order to get the plasma CB increase to 13 mg/dl seen in biliary atresia, it is necessary to reduce R_{Bile} to 0.02 of its normal value. [Figure 2](#) shows a plot of plasma UB and CB versus the fractional reduction in R_{Bile} . The model predicts that, for pure CB pathologies, the increase in plasma UB levels off at about 2 mg/dl as R_{Bile} goes to zero. This is because we have assumed that the plasma UB in rotor syndrome of 2 mg/dl corresponds to the case where OATP is completely knocked out and since the only effect of the increased CB on UB in the model is the competitive inhibition of OATP, this is the maximum predicted UB for CB pathologies. As discussed below, to reach UB concentrations greater than 2 mg/dl, there must also be some UB pathology.

For the mild "pure" UB pathologies in [Table 1](#) such as Gilbert's syndrome, the plasma UB increases 5.2-fold to 1.84 mg/dl, with no significant increase in plasma CB. This is simulated in the model ([Figure 1](#)) by a decrease in the rate of glucuronidation of UB, characterized by a decrease in the rate constant R_{Glu} (eq. (5)). [Table 4](#) lists the model values of

Table 3 Model Plasma UB and CB Concentrations for Different Pathological Fractional Decreases in the Biliary Secretion Rate Constant (R_{Bile})

Fractional Decrease in R_{Bile}	Plasma UB (mg/dl)	Plasma CB (mg/dl)
1.0 (Normal)	0.35	0.012
0.1	0.59	0.23
0.05	1.27	1.77
0.046	1.39	2.42
0.04	1.58	3.82
0.03	1.72	7.1
0.02	1.81	12.9

UB and CB for a range of reductions in R_{Glu} . The plasma UB seen in Gilbert's is reproduced by 0.072 (14-fold) fractional reduction. There is only a very small corresponding model increase in CB, in agreement with the clinical observations (Table 1). Reproducing the 53-fold increase of UB to 18.4 mg/dl seen in Crigler-Najjar (Table 1) requires a 0.014 (71-fold) fractional reduction in R_{Glu} .

The increased plasma bilirubin associated with hemolytic anemia (Table 1) also represents a pure UB pathology. It represents, presumably, simply an increase in the rate of total UB production, characterized by the rate constant M in Figure 1. Table 5 lists the plasma UB and CB concentrations for a range of increases of M . The hemolytic anemia UB value in Table 1 of 1.46 mg/dl is produced in the model by a 2.7-fold increase in M , with a corresponding increase of plasma CB to 0.058 mg/dl, identical to what is observed clinically (Table 1). This 2.7-fold increase in bilirubin production ($= M$) is similar to the directly measured increased values of bilirubin production in chronic hemolytic anemia reported by Berk et al¹⁷

Model Description of Alcoholic Cirrhosis

The above discussions for the "pure" UB or CB pathologies focus on the relatively rare genetic defects in specific bilirubin metabolic pathways that can be easily related to a single model rate constant (eg, R_{Glu} , R_{Bile} , M). However, the

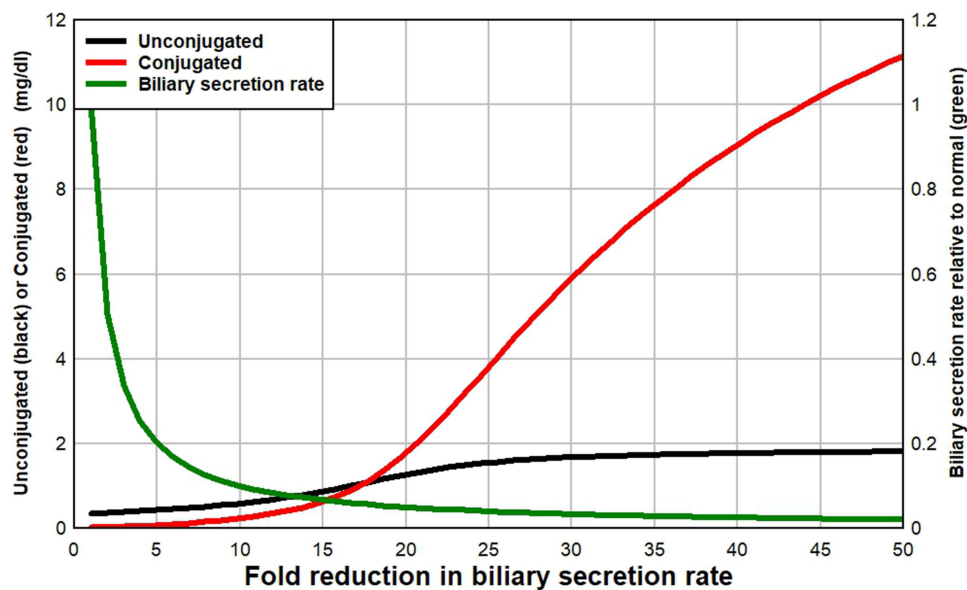


Figure 2 Plasma UB (black) and CB (red) concentration as function of the relative decrease in biliary secretion rate (R_{Bile} , green). The normal condition is for $x=1$ fold reduction, and $x = 50$ corresponds to a R_{Bile} of 1/50th of normal. The fractional reduction of the biliary secretion rate (green) is indicated on the right side of the graph.

Table 4 Model Plasma UB and CB Concentrations for Different Pathological Fractional Decreases in the Rate of UB Glucuronidation (RGlu)

Fraction Decrease in RGlu	Plasma UB (mg/dl)	Plasma CB (mg/dl)
1.0 (Normal)	0.35	0.012
0.2	0.69	0.014
0.1	1.25	0.018
0.072	1.84	0.022
0.05	3.03	0.03
0.03	6.57	0.054
0.014	19.0	0.137

Table 5 Model Plasma UB and CB Concentration for Pathological Increases in the Rate of Bilirubin Production (M)

Fraction Increase in M	Plasma UB (mg/dl)	Plasma CB (mg/dl)
1.0 (Normal)	0.35	0.012
1.50	0.60	0.021
2.0	0.91	0.033
2.7	1.49	0.058
3.0	1.81	0.07
4.0	3.13	0.145
5.0	4.85	0.26
6.0	6.81	0.44

much more common clinical cause of increased plasma bilirubin is non-specific generalized liver disease, represented in [Table 1](#) by alcoholic cirrhosis. One of the questions posed in the Introduction is what mechanism in cirrhosis can produce the roughly equal plasma UB and CB concentrations (≈ 3 mg/dl), requiring a 250 increase in CB, versus only an 8.4-fold increase in UB. One possibility is that cirrhosis simply represents bulk hepatic cell dysfunction, reducing all 5 of the model cellular rate constants (V_M , P , R_{MRP} , R_{Bile} , R_{Glu}) by the same fraction, equal to the remaining fraction of living cells. However, this reduction is clearly not representative of what is seen clinically in cirrhosis. For example, a five-fold reduction in all the rate constants (80% cell death) results in a model plasma UB of 4.79 mg/dl and CB of 0.244 mg/dl, far different than the roughly equal UB and CB values that are characteristic of cirrhosis. In order to match the CB and UB values observed in cirrhosis, it is necessary to selectively decrease some rate constants more than others. In the following, we will discuss one set of values that accomplishes this.

Hur and Park¹⁸ have published a scatter plot of more than 4000 measurements of UB and CB, along with regression equations for CB versus total bilirubin (= UB + CB) for various cholestatic conditions, including alcoholic cirrhosis. We used the fit of our model to their regression equation for alcoholic cirrhosis as the criterion for the quality of the model fit. Through trial-and-error adjustments of the 5 model rate constants, we found an

approximate fit to this regression using the following functional decreases in the 5 rate coefficients as a function of the “fractional impairment parameter” F_R :

$$R_{Bile} = F_R R_{Bile0} \quad V_M = F_R V_{M0} \quad R_{Glu} = \kappa F_R R_{Glu0} \quad R_{MRP} = \kappa F_R R_{MRP0} \quad P = \kappa F_R P_0 \quad (15)$$

$$\kappa = \frac{8}{1 + 7 F_R} \quad (16)$$

where R_{Bile0} , V_{M0} , R_{Glu0} , R_{MRP0} , and P_0 are the normal values listed in Table 2. The rate constants whose decreases directly produce an increase in CB (V_M , R_{Bile}) decrease by the factor F_R , while the other rate constants decrease by a smaller amount determined by the parameter κ (eq. (16)). For example, for an F_R of 0.1, V_M and R_{Bile} are decreased by a factor 10, while the other rate constants are only decreased by a factor of 2.125. Figure 3 shows a plot of the plasma UB and CB as a function of $1/F_R$ and Table 6 lists some specific values. Over a wide range of pathological plasma UB and CB concentrations (3 to 12 mg/dl), UB and CB are roughly equal with CB somewhat greater than UB at high bilirubin levels, as is characteristic of alcoholic cirrhosis.

Figure 4 is a plot of the model values of CB versus Total (CB + UB) plasma bilirubin for the model alcoholic cirrhosis values plotted in Figure 3. The dashed red line is the clinical regression relation for alcoholic cirrhosis reported by Hur and Park.¹⁸ The agreement between the model prediction and clinical values is quite good, except at the highest total bilirubin values. This deviation at high values could possibly be explained by the presence δ -bilirubin, which results from the covalent linkage of CB with albumin. δ -bilirubin is cleared at a much slower rate than CB so that, in long-standing CB hyperbilirubinemia, it can account for as much as 40% of the CB.² The fit could also certainly be improved with further adjustment of the relative variation of the 5 model rate constants, in place of the relatively simple relations we used in eqs. (15) and (16).

Considerations of the Experimental Bases for the Model Assumptions

Although there has been an enormous research effort devoted to understanding the regulation of plasma bilirubin concentrations, we believe that we are presenting the first proposal of a detailed kinetic model that can quantitatively account for the main observations of the changes in plasma UB and CB in hepatic pathologies. In this section, we will briefly discuss what, if any, are the experimental bases for the model’s assumptions. There are five major assumptions: 1) Normally, there must be a high rate of efflux of CB from the hepatocyte to the plasma; 2) This efflux must be balanced by

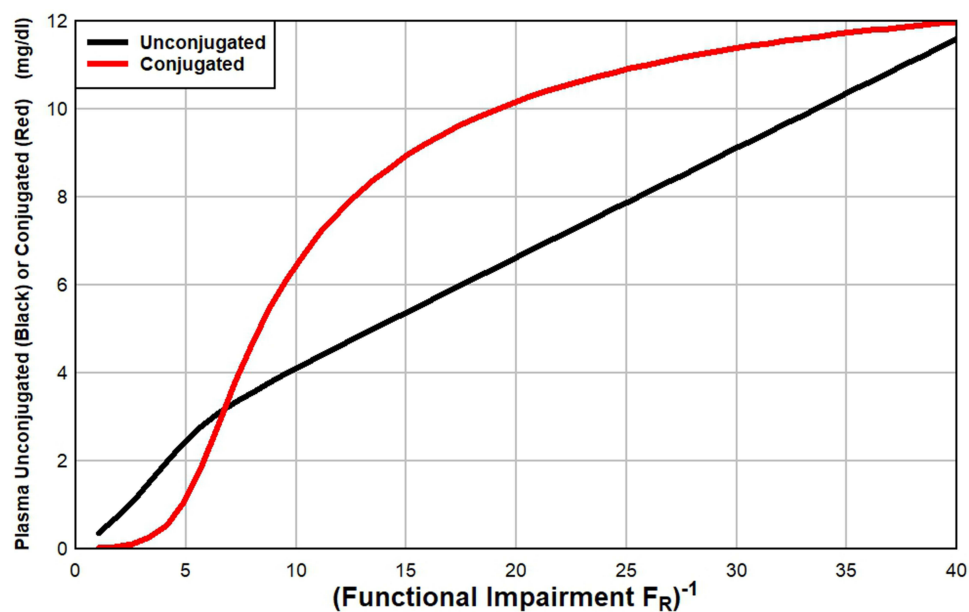


Figure 3 Model simulation of alcoholic cirrhosis. The plasma unconjugated (black) or conjugated (red) bilirubin (mg/dl) is plotted as a function of the inverse of the functional impairment parameter (F_R). The value of $F_R = 1$ corresponds to the normal state.

Table 6 Increase in Plasma UB and CB (mg/dl) Concentration as the Functional Impairment Parameter FR Decreases from 1 (Normal) to 0.025, Simulating Alcoholic Cirrhosis. The Corresponding Reductions in the 5 Model Rate Constants (V_M , R_{Bile} , P , R_{Glu} , R_{MRP}) are Listed in the Second and Third Columns

Functional Impairment (FR)	Fractional Reduction of V_M and R_{Bile}	Fractional Reduction of P , R_{Glu} , and R_{MRP}	Plasma UB (mg/dl)	Plasma CB (mg/dl)
1.0 (Normal)	1.0	1.0	0.35	0.02
0.5	0.5	0.89	0.79	0.060
0.2	0.2	0.67	2.45	1.125
0.15	0.1	0.58	3.15	3.08
0.1	0.1	0.47	4.1	6.45
0.05	0.05	0.30	6.62	10.17
0.025	0.025	0.17	11.6	12.0

a rapid rate of cell uptake (presumably by OATP) to maintain the very low plasma CB of healthy subjects; 3) This uptake must saturate as CB rises, blocking CB uptake and producing the huge plasma CB increases observed in a variety of conditions; 4) UB must also be competitively transported by this transporter (OATP) so that CB saturation also inhibits the rate of UB uptake, explaining the plasma UB increases that are observed in pure CB pathologies; And, finally, 5) There must be an alternative UB uptake pathway (eg, J_P , Figure 1) to account for the limited increase in plasma UB that is observed in Rotor syndrome when OATP is, presumably, completely knocked out.

The key experimental result supporting the model is the observation that double knock-out of OATP1A and OATP1B in the mouse produces a 400-fold increase in plasma CB along with a smaller (2.5-fold) increase in plasma UB.¹³ The obvious explanation for the CB elevations is that there is a normal large rate of recycling of CB with plasma CB normally kept at very low plasma levels by OATP transport. The recognition that subjects with Rotor syndrome have simultaneous

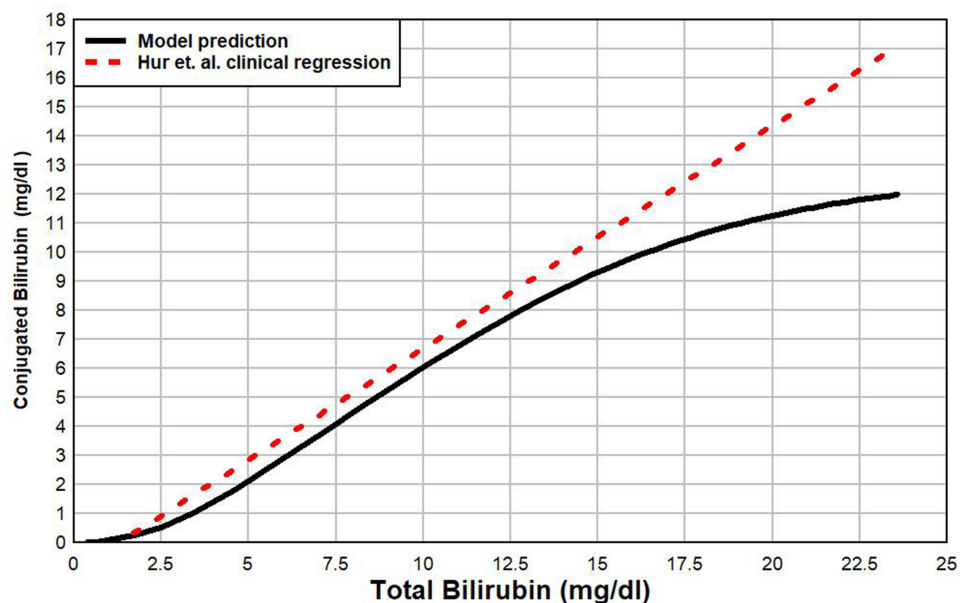


Figure 4 Plot of the conjugated bilirubin versus total bilirubin for increasing severity of alcoholic cirrhosis. The black line is the model prediction, and the red dashed line is the clinical regression relation of Hur and Park.

complete deficiencies in the analogous human genes OATP1B1 and OATP1B3¹⁹ provides an experimental tool for quantitating this normal rate of CB recycling. As shown in eq. (12), in the absence of OATP, the CB efflux must be balanced by the known renal clearance, allowing quantitation of this efflux rate ($= R_{MRP}CB_c$, eq. (12)). The rapid rate of CB uptake determined by this modeling approach is quantitatively similar to that obtained from direct measurements of the human liver clearance of both labeled and unlabeled CB.^{20,21}

The identity of the hepatic efflux CB pathway is less certain. It is probably a protein-mediated active transport system since the efflux occurs in the presence of relatively high plasma CB concentrations. The observation that in mice with a double knock-out of OATP1A and OATP1B, the additional knockout of MRP3 reduced plasma CB by 50%¹³ indicates that MRP3 is, at least, a contributor to this pathway. Although we have arbitrarily identified this CB efflux pathway with MRP3 in our model (Figure 1), the validity of the model does not depend on the molecular identification of this efflux pathway.

The value of the CB K_m of OATP is a critical parameter in the model because it determines the plasma CB concentration range where OATP uptake becomes saturated. The K_m of mouse OATP1B1 for the monoglucuronide is 0.0058 mg/dl. Since this K_m is measured in the absence of albumin binding, to convert it to the K_{CB} of the model requires correcting for albumin binding and extrapolating from the mouse to the analogous human proteins, which is uncertain. We assumed a $K_{CB} = 0.2$ mg/dl.

An essential aspect of the model is that UB and CB are competing for OATP transport, accounting for the increased plasma UB in pure CB pathologies (Table 1). The experimental evidence for this is equivocal. Although Cui et al¹⁵ reported that UB was transported by OATP in an in vitro cell system, Wang et al²² could not confirm this. There is less direct evidence supporting UB transport by OATP. In an older paper, Shupeck et al²¹ report that a high concentration of plasma UB markedly inhibits the hepatic uptake of CB in the rat. Campbell et al²³ provide evidence that inhibition of OATP by drugs such as indinavir and rifamycin is a likely explanation for clinical drug-induced unconjugated hyperbilirubinemia. In a more recent comprehensive review, Keppler²⁴ summarizes a large set of observations that "... support the conclusion that the uptake of UB in human hepatocytes is mediated by members of the OATP family". The model value of the OATP K_m for UB ($K_{UB} = 1.38$ mg/dl) is directly calculated from the assumed value of K_{CB} and the other model parameters (see eq. (14)).

Another model assumption is the existence of a second, lower affinity, UB uptake pathway that can account for the UB uptake in Rotor syndrome when OATP is knocked out. We have assumed (Figure 1) that this is a passive diffusive pathway, for which there is indirect evidence,^{25–27} with the uptake rate proportional to the UB concentration difference across the cell membrane (eq. (2)). Whatever the mechanism, this uptake must be dependent on the cellular UB ($=UB_c$) because the model assumes that the increased UB_c in pure UB pathologies (ie, Gilbert's, Crigler Najjar) decreases the rate of hepatic UB uptake, accounting for the observed increase in plasma UB.

The pathological mechanism(s) producing the increased plasma UB and CB in alcoholic cirrhosis is poorly understood and rarely discussed. As noted above, to explain the relatively similar absolute plasma UB and CB values (requiring approximately a 250-fold increase in CB versus an 8-fold increase in UB), an essential model requirement is that some hepatic processes are more affected than others in cirrhosis. For example, as described in Table 6, for moderate cirrhosis (total bilirubin = 3.6 mg/dl, $F_R = 0.2$) the model requires an 80% decrease in the OATP transport rate (V_M), but only a 37% reduction in both the MRP transport (R_{MRP}) and the glucuronidation rate (R_{Glu}). There is some direct experimental quantitative support for this. Wang et al²⁸ measured tissue expression of various hepatic cell transporters in cirrhosis and reported that OAT1B3 expression was reduced 80%, while there was actually a 34% increase (not decrease) in MRP3 expression. These measurements are per gram of liver, and therefore, the increased MRP3 expression represents an increase per surviving cells, not an absolute increase. Similarly, Macgilchrist²⁹ found that the clearance of indocyanine green (which is transported by OATP³⁰) was reduced 80% in alcoholic cirrhosis, while the clearance of midazolam (which is a function of P450 metabolism) was only reduced by 40%.

Discussion and Conclusions

The clinician commonly attributes an elevated plasma UB concentration to excessive bilirubin production (hemolysis) or diminished glucuronidation (Gilbert's syndrome), while failure to excrete the conjugated product of this reaction somehow results in an elevated plasma CB. Since these two processes are seemingly independent of each other, one might expect that plasma UB and CB might increase in a totally independent fashion. However, as we have discussed at

length, there are multiple conditions in which the plasma concentrations of both CB and UB are elevated in a consistent fashion that would be unlikely to occur if these values were determined independently. The best example is the roughly comparable CB and UB values observed in hepatocellular disease (eg, alcoholic cirrhosis) – a finding that requires an initial massive increase (about 40-fold) in plasma CB to reach the level of UB and then, as liver function further deteriorates, there must be similar increases in the two forms of bilirubin to maintain the 50–50 distribution of CB and UB in the plasma. Such a relationship of plasma CB and UB seems highly unlikely if their plasma concentrations were controlled by independent mechanisms. Despite the enormous research effort directed towards unraveling the pathophysiology of plasma CB and UB elevations, we are unaware of previous discussions of the possibility that the plasma concentration of one form of bilirubin influences the concentration of its counterpart.

In this manuscript, we attempted to devise a model of bilirubin pharmacokinetics that could explain the observed elevations of CB and UB that occur in a wide variety of conditions. An important aspect of this model is that the two species of bilirubin share a common uptake mechanism (OATP) that becomes saturated at relatively low plasma CB concentrations. Thus, a rising concentration of plasma CB slows the hepatic uptake of UB, accounting for the linkage between the plasma concentrations of the two species of bilirubin in hepatocellular disease and other conditions.

Our model (Figure 1) is clearly a very crude simplification of the complex hepatocellular processes. We believe that it represents the bare minimum required to describe bilirubin metabolism, characterized by 5 rate constants (V_M , P , R_{MRP} , R_{Bile} , R_{Glu}) and two binding constants (K_{UB} , K_{CB}), most of which are either determined or highly constrained by experimental and clinical measurements (see Table 2). Our only test of the model is its ability to describe the clinical changes in plasma UB and CB in various pathological conditions. The major limitation in the modeling is the lack of quantitative measurements of the intrahepatic CB and UB concentrations both in normal and in various pathologies. It is our hope that this discussion will provide a stimulus for additional studies that might provide a more direct measurement of these parameters and their pathological changes.

Abbreviations

UB, unconjugated bilirubin; CB, conjugated bilirubin.

Funding

No external funding.

Disclosure

No competing financial or non-financial interests.

References

1. Van den Bergh AAH. La Recherche de la Bilirubine dans le plasma sanguin par la methode de la reaction diazoique. *La Presse Medicale*. 1921;45(4):441.
2. Levitt DG, Levitt MD. Quantitative assessment of the multiple processes responsible for bilirubin homeostasis in health and disease. *Clin Exp Gastroenterol*. 2014;7:307–328. doi:10.2147/CEG.S64283
3. Muraca M, Fevery J, Blanckaert N. Relationships between serum bilirubins and production and conjugation of bilirubin. Studies in Gilbert's syndrome, Crigler-Najjar disease, hemolytic disorders, and rat models. *Gastroenterology*. 1987;92(2):309–317. doi:10.1016/0016-5085(87)90123-5
4. Dumas BT, Wu TW. The measurement of bilirubin fractions in serum. *Critical Rev Clin Lab Sci*. 1991;28(5–6):415–445. doi:10.3109/10408369109106872
5. Lee HA, Jung JY, Lee YS, et al. Direct Bilirubin Is More Valuable than Total Bilirubin for Predicting Prognosis in Patients with Liver Cirrhosis. *Gut Liver*. 2021;15(4):599–605. doi:10.5009/gnl20171
6. Al-Jumaily EF, Faiha'a MK. The Effect of Chronic Liver Diseases on Some Biochemical Parameters in Patients Serum. *Curr Res J Biol Sci*. 2012;4.
7. Shani M, Seligsohn U, Gilon E, Sherba C, Adam A. Dubin-Johnson syndrome in Israel. I. Clinical, laboratory and genetic aspects in 101 cases. *Quart J Med*. 1970;39(156):549.
8. Namihisa T, Yamaguchi K. The constitutional hyperbilirubinemia in Japan. Studies on the 139 cases reported during the period 1963 to 1969. *Gastroenterologia Japonica*. 1973;8(4):311–321. doi:10.1007/BF02779108
9. Sieg A, Konig R, Ullrich D, Fevery J. Subfractionation of serum bilirubins by alkaline methanolysis and thin-layer chromatography. An aid in the differential diagnosis of icteric diseases. *J Hepatol*. 1990;11(2):159–164. doi:10.1016/0168-8278(90)90107-3
10. Cameron JL, Filler RM, Iber FL, Abei T, Randolph JG. Metabolism and excretion of C14-labeled bilirubin in children with biliary atresia. *New Engl J Med*. 1966;274(5):231–236. doi:10.1056/NEJM196602032740501

11. Castano G, Lucangioli S, Sookoian S, et al. Bile acid profiles by capillary electrophoresis in intrahepatic cholestasis of pregnancy. *Clin Sci (Lond)*. 2006;110(4):459–465. doi:10.1042/CS20050302
12. Raedsch R, Lauterburg BH, Hofmann AF. Altered bile acid metabolism in primary biliary cirrhosis. *Dig Dis Sci*. 1981;26(5):394–401. doi:10.1007/BF01313580
13. van de Steeg E, Wagenaar E, van der Kruijssen CM, et al. Organic anion transporting polypeptide 1a/1b-knockout mice provide insights into hepatic handling of bilirubin, bile acids, and drugs. *J Clin Invest*. 2010;120(8):2942–2952. doi:10.1172/JCI42168
14. Iusuf D, van de Steeg E, Schinkel AH. Functions of OATP1A and 1B transporters in vivo: insights from mouse models. *Trends Pharmacol Sci*. 2012;33(2):100–108. doi:10.1016/j.tips.2011.10.005
15. Cui Y, Konig J, Leier I, Buchholz U, Keppler D. Hepatic uptake of bilirubin and its conjugates by the human organic anion transporter SLC21A6. *J Biol Chem*. 2001;276(13):9626–9630. doi:10.1074/jbc.M004968200
16. Fulop M, Sandson J, Dialyzability BP. Protein Binding, and Renal Excretion of Plasma Conjugated Bilirubin. *J Clin Invest*. 1965;44(4):666–680. doi:10.1172/JCI105179
17. Berk PD, Rodkey FL, Blaschke TF, Collison HA, Waggoner JG. Comparison of plasma bilirubin turnover and carbon monoxide production in man. *J Lab Clin Med*. 1974;83(1):29–37.
18. Hur K, Park I. Clinical usefulness of the direct/total bilirubin ratio. *Lab Med Online*. 2018;8(4):127–134. doi:10.3343/lmo.2018.8.4.127
19. van de Steeg E, Stranecky V, Hartmannova H, et al. Complete OATP1B1 and OATP1B3 deficiency causes human Rotor syndrome by interrupting conjugated bilirubin reuptake into the liver. *J Clin Invest*. 2012;122(2):519–528. doi:10.1172/JCI59526
20. Arias IM, Johnson L, Wolfson S. Biliary excretion of injected conjugated and unconjugated bilirubin by normal and Gunn rats. *A J Physiol*. 1961;200(5):1091–1094. doi:10.1152/ajplegacy.1961.200.5.1091
21. Shupeck M, Wolkoff AW, Scharschmidt BF, Waggoner JG, Berk PD. Studies of the kinetics of purified conjugated bilirubin-3H in the rat. *Am J Gastroenterol*. 1978;70(3):259–264.
22. Wang P, Kim RB, Chowdhury JR, Wolkoff AW. The human organic anion transport protein SLC21A6 is not sufficient for bilirubin transport. *J Biol Chem*. 2003;278(23):20695–20699. doi:10.1074/jbc.M301100200
23. Campbell SD, de Morais SM, Xu JJ. Inhibition of human organic anion transporting polypeptide OATP 1B1 as a mechanism of drug-induced hyperbilirubinemia. *Chem Biol Interact*. 2004;150(2):179–187. doi:10.1016/j.cbi.2004.08.008
24. Keppler D. The roles of MRP2, MRP3, OATP1B1, and OATP1B3 in conjugated hyperbilirubinemia. Drug metabolism and disposition: the biological fate of chemicals. *Apr*. 2014;42(4):561–565. doi:10.1124/dmd.113.055772
25. Iga T, Eaton DL, Klaassen CD. Uptake of unconjugated bilirubin by isolated rat hepatocytes. *A J Physiol*. 1979;236(1):C9–C14. doi:10.1152/ajpcell.1979.236.1.C9
26. Zucker SD, Goessling W, Hoppin AG. Unconjugated bilirubin exhibits spontaneous diffusion through model lipid bilayers and native hepatocyte membranes. *J Biol Chem*. 1999;274(16):10852–10862. doi:10.1074/jbc.274.16.10852
27. Jones EA, Shrager R, Bloomer JR, Berk PD, Howe RB, Berlin NI. Quantitative studies of the delivery of hepatic-synthesized bilirubin to plasma utilizing -aminolevulinic acid-4- 14 C and bilirubin- 3 H in man. *J Clin Invest*. 1972;51(9):2450–2458. doi:10.1172/JCI107058
28. Wang L, Collins C, Kelly EJ, et al. Transporter Expression in Liver Tissue from Subjects with Alcoholic or Hepatitis C Cirrhosis Quantified by Targeted Quantitative Proteomics. *Drug Metab Disposition*. 2016;44(11):1752–1758. doi:10.1124/dmd.116.071050
29. MacGilchrist AJ, Birnie GG, Cook A, et al. Pharmacokinetics and pharmacodynamics of intravenous midazolam in patients with severe alcoholic cirrhosis. *Gut*. 1986;27(2):190–195. doi:10.1136/gut.27.2.190
30. de Graaf W, Hausler S, Heger M, et al. Transporters involved in the hepatic uptake of (99m)Tc-mebrofenin and indocyanine green. *J Hepatol*. 2011;54(4):738–745. doi:10.1016/j.jhep.2010.07.047

Clinical and Experimental Gastroenterology

Dovepress

Publish your work in this journal

Clinical and Experimental Gastroenterology is an international, peer-reviewed, open access, online journal publishing original research, reports, editorials, reviews and commentaries on all aspects of gastroenterology in the clinic and laboratory. This journal is indexed on American Chemical Society's Chemical Abstracts Service (CAS). The manuscript management system is completely online and includes a very quick and fair peer-review system, which is all easy to use. Visit <http://www.dovepress.com/testimonials.php> to read real quotes from published authors.

Submit your manuscript here: <https://www.dovepress.com/clinical-and-experimental-gastroenterology-journal>